The effect of plasma flow, compressibility, and Landau damping on resistive wall modes

C. N. Lashmore-Davies, J. A. Wesson, and C. G. Gimblett

Citation: Phys. Plasmas **6**, 3990 (1999); doi: 10.1063/1.873674
View online: http://dx.doi.org/10.1063/1.873674
View Table of Contents: http://pop.aip.org/resource/1/PHPAEN/v6/i10
Published by the American Institute of Physics.

The effect of plasma flow, compressibility, and Landau damping on resistive wall modes

C. N. Lashmore-Davies
EURATOM/UKAEA Fusion Association, Culham Science Centre, Abingdon, Oxon, OX14 3DB, United Kingdom

J. A. Wesson
JET Joint Undertaking, Abingdon, OX14 3EA, United Kingdom

C. G. Gimblett
EURATOM/UKAEA Fusion Association, Culham Science Centre, Abingdon, Oxon, OX14 3DB, United Kingdom

(Received 22 February 1999; accepted 16 June 1999)

A uniform compressible plasma with a uniform flow along the magnetic field in the presence of a resistive wall is shown to be subject to two instabilities. For the first instability, the flow velocity is required to exceed the Alfvén speed, whereas for the second it need only exceed the sound speed. For a sufficiently high ion temperature, ion Landau damping is shown to stabilize the second instability associated with the sound speed. [S1070-664X(99)03910-5]

I. INTRODUCTION

The subject of resistive wall modes has become of increasing interest in view of its relevance to the prospects of advanced tokamaks. Since the observation of greater stability to this mode on DIII-D in the presence of toroidal flow,[1] various attempts[2–7] have been made to find a stabilizing mechanism due to rotation.

In order to clarify the effect of flow, Wesson[8] has recently analyzed a simple model consisting of the uniform flow of an incompressible fluid along a uniform magnetic field in slab geometry. The fluid was assumed to be separated from a thin, resistive wall by a vacuum region, with a further vacuum region beyond the resistive wall. In this model the only source of free energy is the plasma flow. It was shown that a resistive wall instability occurred when the flow velocity, v_0, exceeded a critical velocity, i.e., $v_0 > \sqrt{2}c_A$, where c_A is the Alfvén velocity. The existence of a critical velocity, $v_0 \sim c_A$, in the above model is due to the fact that, apart from the wall mode, only compressional Alfvén waves are involved. The shear Alfvén wave decouples from the compressional wave in this model. However, a compressible model allows the propagation of the slow magnetosonic wave whose phase velocity, c_s, is much lower than the Alfvén velocity under low beta conditions. In view of this, the analysis given in Ref. 8 has been extended to the case of a compressible plasma.

The compressible model, with the plasma flowing along the equilibrium magnetic field includes the resistive wall instability discussed in Ref. 8, for which the critical flow speed is of the order $\sqrt{2}c_A$. However, an additional resistive wall instability is found which occurs at the much lower critical flow speed, c_s. Toroidal flow speeds of the order of the Alfvén velocity are not relevant to present tokamak conditions. On the other hand, toroidal flows of the order of the sound speed are much closer to observed values.

The ideal magnetohydrodynamic (MHD) model including plasma compressibility contains only undamped fast and slow magnetosonic waves. The condition for sound waves to be weakly damped is that $T_e \gg T_i$. However, under normal tokamak conditions, $T_e \sim T_i$, and sound waves are heavily damped by ion Landau damping. In the final part of the paper kinetic effects are incorporated into the compressible model in order to study the effect of Landau damping on the resistive wall instability arising from the slow magnetosonic wave. It is found that the instability persists for $T_e \gg T_i$ but as T_e/T_i is reduced, the ion Landau damping becomes strong enough to stabilize the instability.

II. THE COMPRESSIBLE MODEL

A plane slab model will again be employed but instead of the semi-infinite plasma used in Ref. 8 a finite slab will be analyzed. The slab is taken to be symmetric as illustrated in Fig. 1. The compressible plasma is described by the equations of ideal MHD. Remembering that we have assumed a uniform flow and equilibrium magnetic field where $\mathbf{B}_0 = (0,0,B_0), \mathbf{v}_0 = (0,0,v_0)$, the linearized equations of ideal MHD can be written,

$$\rho_0 \frac{\partial \mathbf{v}_1}{\partial t} + \rho_0 v_0 \frac{\partial}{\partial z}\mathbf{v}_1 = -\nabla p_1 + (\nabla \times \mathbf{B}_1) \times \frac{\mathbf{B}_0}{\mu_0}, \tag{1}$$

$$\frac{\partial \mathbf{B}_1}{\partial t} = \nabla \times (\mathbf{v}_1 \times \mathbf{B}_0) + \nabla \times (\mathbf{v}_0 \times \mathbf{B}_1), \tag{2}$$

$$\frac{\partial \rho_1}{\partial t} + v_0 \frac{\partial \rho_1}{\partial z} + \rho_0 (\nabla \cdot \mathbf{v}_1) = 0, \tag{3}$$

where equilibrium quantities have a subscript ''0'' and perturbed quantities a subscript ''1.'' The perturbed quantities

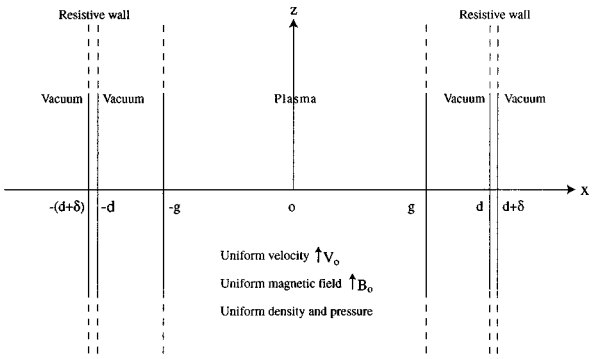

FIG. 1. Symmetric, finite slab configuration in which the plasma, vacuum and resistive wall regions extend to infinity in the y- and z-directions.

will be assumed to have a variation $f(x)\exp i(kz-\omega t)$. With this assumption and also assuming an isothermal equation of state,

$$p_1=c_s^2\rho_1, \tag{4}$$

where c_s is the sound speed, all variables can be expressed in terms of B_{1x} which satisfies the equation

$$\left[\frac{\bar{\omega}^2k^2c_s^2}{(\bar{\omega}^2-k^2c_s^2)}+k^2c_A^2\right]\frac{d^2B_{1x}}{dx^2}+(\bar{\omega}^2-k^2c_A^2)k^2B_{1x}=0, \tag{5}$$

where $\bar{\omega}=\omega-kv_0$. We note, in passing, that the fields v_{1y} and B_{1y} decouple from the present problem. These variables are associated with the shear Alfvén wave, whereas Eq. (5) describes the fast and slow magnetosonic waves. The incompressible result is obtained from Eq. (5) by taking the limit $c_s\to\infty$, when the equation reduces to Eq. (2) of Ref. 8. However, for a low-beta plasma, $c_s\ll c_A$, which is very different from the incompressible limit.

It is convenient to write Eq. (5) in the alternative form,

$$\frac{d^2B_{1x}}{dx^2}+\frac{k^2(\bar{\omega}^2-k^2c_A^2)(\bar{\omega}^2-k^2c_s^2)}{\{\bar{\omega}^2k^2c_s^2+k^2c_A^2(\bar{\omega}^2-k^2c_s^2)\}}B_{1x}=0. \tag{6}$$

III. THE BOUNDARY CONDITIONS

The solution for the perturbed magnetic field, B_{1x} given by Eq. (6) must be matched to the corresponding solutions in the vacuum regions and the resistive wall. The plasma exists in the region $-g\leqslant x\leqslant g$, where the solution is

$$B_{1x}^p=A_+e^{i\beta x}+A_-e^{-i\beta x}, \tag{7}$$

where

$$\beta^2=\frac{(\bar{\omega}^2-k^2c_A^2)(\bar{\omega}^2-k^2c_s^2)}{\bar{\omega}^2c_s^2+c_A^2(\bar{\omega}^2-k^2c_s^2)}. \tag{8}$$

In vacuum, B_{1x} satisfies

$$\frac{d^2B_{1x}}{dx^2}-k^2B_{1x}=0. \tag{9}$$

Hence, in the region $g\leqslant x\leqslant d$,

$$B_{1x}^v=Ce^{kx}+De^{-kx}. \tag{10}$$

Similarly, in the region, $-d\leqslant x\leqslant -g$,

$$B_{1x}^v=Ee^{kx}+Fe^{-kx}. \tag{11}$$

For $x\geqslant d+\delta$, where δ is the thickness of the, thin, resistive wall,

$$B_{1x}^v=Ge^{-kx} \tag{12}$$

and for $x\leqslant -d-\delta$,

$$B_{1x}=He^{kx}. \tag{13}$$

The above fields and their derivatives must be joined across the plasma vacuum interfaces at $x=\pm g$ and the resistive walls at $x=\pm d$. The boundary conditions at a thin resistive wall are[7]

B_{1x} continuous, and

$$\left.\frac{dB_{1x}}{dx}\right|_d^{d+\delta}=\frac{-i\omega}{c_W}B_{1x}, \tag{14}$$

where

$$c_W=(\mu_0\sigma\delta)^{-1}. \tag{15}$$

Turning to the plasma–vacuum interface, B_{1x} is again required to be continuous. The final condition can be obtained by integrating the x-component of Eq. (1) across the interface, giving,

$$p_1+\left.\frac{B_0^p}{\mu_0}B_{1z}\right|_{x=\pm g^-}=\left.\frac{B_0^v}{\mu_0}B_{1z}\right|_{x=\pm g^+}, \tag{16}$$

where the quantities on the left-hand side of the equation refer to the plasma and those on the right-hand side to the vacuum.

We note that since there is an equilibrium pressure discontinuity there will therefore be a jump in B_0 at the plasma vacuum interface. This can be obtained from the equation for the equilibrium pressure balance,

$$\frac{d}{dx}\left(p_0+\frac{B_0^2}{2\mu_0}\right)=0. \tag{17}$$

Integrating Eq. (17) across the plasma–vacuum interface gives,

$$p_0+\frac{(B_0^p)^2}{2\mu_0}=\frac{(B_0^v)^2}{2\mu_0}. \tag{18}$$

$\nabla.\mathbf{B}_1=0$ gives the relation

$$B_{1z}^v=\frac{i}{k}\frac{dB_{1x}^v}{dx}, \tag{19}$$

for the vacuum and a similar result for the plasma,

$$B_{1z}^p=\frac{i}{k}\frac{dB_{1x}^p}{dx}. \tag{20}$$

With the aid of Eqs. (1)–(3), p_1 can also be expressed in terms of B_{1x},

$$p_1=\frac{i\rho_0\bar{\omega}^2c_s^2}{kB_0^p(\bar{\omega}^2-k^2c_s^2)}\frac{dB_{1x}^p}{dx}. \tag{21}$$

Substituting Eqs. (19)–(21) into Eq. (16) gives,

$$\frac{\rho_0\overline{\omega}^2c_s^2}{kB_0^p(\overline{\omega}^2-k^2c_s^2)}\frac{dB_{1x}^p}{dx}+\frac{B_0^p}{\mu_0 k}\frac{dB_{1x}^p}{dx}\bigg|_{x=\pm g^-}$$

$$=\frac{B_0^v}{\mu_0 k}\frac{dB_{1x}^v}{dx}\bigg|_{x=\pm g^+}. \tag{22}$$

For low beta, with $2\mu_0 p_0 \ll (B_0^p)^2$, Eq. (18) can be written

$$B_0^v \simeq B_0^p\left[1+\frac{\mu_0 p_0}{(B_0^p)^2}\right]. \tag{23}$$

Substituting Eq. (23) into Eq. (22), the final form of the second plasma–vacuum interface boundary condition is

$$\left[\frac{\overline{\omega}^2c_s^2}{(\overline{\omega}^2-k^2c_s^2)}+c_A^2\right]\frac{dB_{1x}^p}{dx}\bigg|_{x=\pm g^-}=(c_A^2+c_s^2)\frac{dB_{1x}^v}{dx}\bigg|_{x=\pm g^+}. \tag{24}$$

IV. THE DISPERSION RELATION

Applying the boundary conditions given in the previous section, the dispersion relation can be written as

$$X^2e^{2i\beta g}-Y^2e^{-2i\beta g}=0, \tag{25}$$

where

$$X=\frac{Fi\beta}{k}-(c_A^2+c_s^2)G_c, \tag{26}$$

$$Y=\frac{Fi\beta}{k}+(c_A^2+c_s^2)G_c, \tag{27}$$

$$F=\frac{\overline{\omega}^2c_s^2}{(\overline{\omega}^2-k^2c_s^2)}+c_A^2, \tag{28}$$

and

$$G_c=\frac{\{e^{-2k(d-g)}+(1+(2ikc_W/\omega))\}}{\{e^{-2k(d-g)}-(1+(2ikc_W/\omega))\}}. \tag{29}$$

Clearly, Eq. (25) can be factorized into two independent dispersion relations,

$$Xe^{i\beta g}-Ye^{-i\beta g}=0 \tag{30}$$

and

$$Xe^{i\beta g}+Ye^{-i\beta g}=0. \tag{31}$$

A physical distinction between the two dispersion relations given by Eqs. (30) and (31) can be obtained as follows. The solution for the perturbed magnetic field component, B_{1x}^p, in the plasma is given by Eq. (7). The value of this quantity at the origin is

$$B_{1x}^p(0)=A_+ +A_- \tag{32}$$

and its derivative is

$$\frac{dB_{1x}^p(0)}{dx}=i\beta(A_+ -A_-). \tag{33}$$

By imposing the boundary conditions, en route to obtaining the dispersion relation, Eq. (25), the following relation between A_+ and A_- can be found

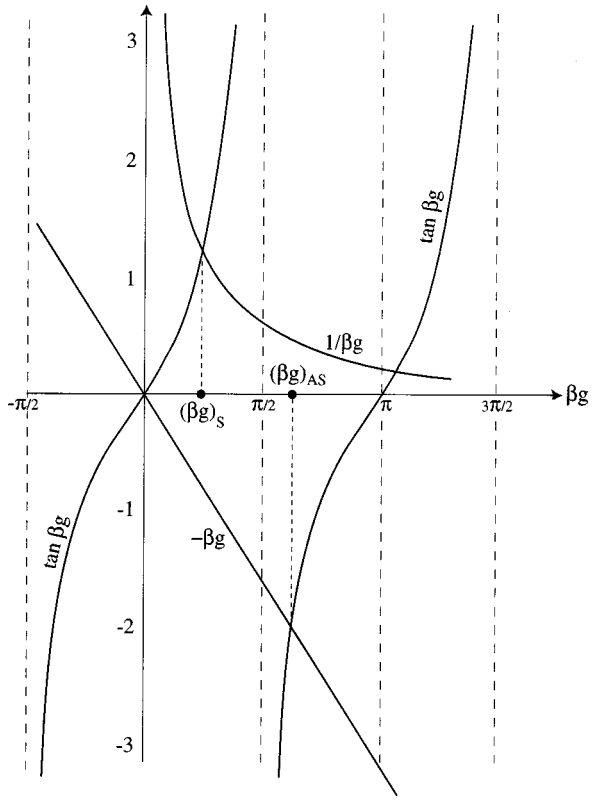

FIG. 2. Graphical solutions of the symmetric, Eq. (43), and antisymmetric, Eq. (45), marginal stability conditions. $(\beta g)_S$ is the root of the symmetric equation and $(\beta g)_{AS}$ the antisymmetric root.

$$A_-=\frac{YA_+}{X}e^{-2i\beta g}. \tag{34}$$

With the aid of this relation, Eqs. (32) and (33) can be written

$$B_{1x}^p(0)=\frac{A_+}{X}e^{-i\beta g}(Xe^{i\beta g}+Ye^{-i\beta g}), \tag{35}$$

$$\frac{dB_{1x}^p(0)}{dx}=\frac{i\beta A_+}{X}e^{-i\beta g}(Xe^{i\beta g}-Ye^{-i\beta g}). \tag{36}$$

Hence, the dispersion relation given by Eq. (30) describes modes for which the perturbed magnetic field B_{1x} is symmetric $(dB_{1x}^p(0)/dx=0)$ about the origin whilst Eq. (31) describes modes for which B_{1x}^p is antisymmetric $(B_{1x}(0)=0)$.

With the aid of Eqs. (8) and (26)–(28), and noting that $F=(\overline{\omega}^2-k^2c_A^2)/\beta^2$, Eqs. (30) and (31) can be written

$$-\frac{\beta k}{(\overline{\omega}^2-k^2c_A^2)}=\frac{\tan\beta g}{G_c(c_A^2+c_s^2)}(\text{SYMMETRIC}) \tag{37}$$

and

$$\frac{(\overline{\omega}^2-k^2c_A^2)}{\beta k}=G_c(c_A^2+c_s^2)\tan\beta g(\text{ANTISYMMETRIC}). \tag{38}$$

The physical content of the dispersion relations given by Eqs. (37) and (38) can be best understood by considering various approximate solutions.

A. Alfvén wave case

Assuming that $\bar{\omega} \sim kc_A$, $v_0 \sim c_A$ and using the low-beta condition $c_s \ll c_A$, Eq. (8) is approximated by

$$\beta^2 \simeq \frac{(\bar{\omega}^2 - k^2 c_A^2)}{c_A^2}. \tag{39}$$

Substituting Eq. (39) into Eq. (37) and neglecting c_s^2 in comparison to c_A^2, the symmetric dispersion relation is approximated by

$$-\frac{kg}{\beta g} = \frac{\tan \beta g}{G_c}. \tag{40}$$

Substituting Eq. (29) for G_c into Eq. (40), the dispersion relation can be expressed in the form

$$\left\{[1+e^{-2k(d-g)}]\frac{kg}{\beta g} - [1-e^{-2k(d-g)}]\tan \beta g\right\}\omega = -2ikc_w\left(\frac{kg}{\beta g} - \tan \beta g\right). \tag{41}$$

In general, the ω-solution to Eq. (41) is $\omega = \omega_r + i\gamma$. Since all the parameters in Eq. (41) are real, except for the wall term ikc_w, it is clear that the marginal condition, $\gamma = 0$, can only be satisfied when $\omega_r = 0$. For values of ω close to the marginal solution, Eq. (41) can be solved approximately as

$$\omega \simeq \frac{-2ikc_W[(kg/\beta g) - \tan \beta g]}{[1+e^{-2k(d-g)}]\{(kg/\beta g) - ([1-e^{-2k(d-g)}]/[1+e^{-2k(d-g)}])\tan \beta g\}}, \tag{42}$$

The stability threshold condition, $\omega = 0$, is given from Eq. (42),

$$\frac{kg}{\beta g} - \tan \beta g = 0. \tag{43}$$

Similarly, the solution to the antisymmetric dispersion relation for values of ω close to the marginal value is

$$\omega \simeq \frac{-2ikc_W[(\beta g/kg) + \tan \beta g]}{[1-e^{-2k(d-g)}]\{(\beta g/kg) + ([1+e^{-2k(d-g)}]/[1-e^{-2k(d-g)}])\tan \beta g\}}. \tag{44}$$

Hence, the threshold condition for the antisymmetric modes is

$$\frac{\beta g}{kg} + \tan \beta g = 0. \tag{45}$$

The solutions to Eqs. (43) and (45) are shown graphically in Fig. 2 for the condition $kg = 1$. For the symmetric mode the solution is given, approximately as $\beta g \simeq 0.86$. Using Eq. (39), this yields

$$v_0 \simeq 1.3 c_A, \tag{46}$$

which is near to the marginal condition $v_0 = \sqrt{2} c_A$ given in Ref. 8. The solution of Eq. (45) for the antisymmetric modes is $\beta g \simeq 2$ which yields

$$v_0 = \sqrt{5} c_A. \tag{47}$$

Returning to Eqs. (42) and (44), we consider values of βg close to the marginal values given by Eqs. (43) and (45). It can be seen from Eq. (42) that for βg slightly above the threshold value, Im $\omega > 0$, i.e., the symmetric mode becomes unstable with a growth rate proportional to kc_W. Similarly, the antisymmetric mode is unstable for values of βg slightly above the threshold value given by Eq. (45) and again the growth rate is proportional to kc_W. Note also that as βg continues to increase, the growth rate of both the symmetric and antisymmetric modes formally tends to infinity as the denominators in Eqs. (42) and (44) tend to zero. Clearly the approximations break down before this condition is reached.

The significance of this behavior is examined by treating the dispersion relations perturbatively. Consider the symmetric dispersion relation given by Eq. (40). Expanding Eq. (29) for $kc_W/\omega \ll 1$ we obtain

$$G_c \simeq -F_c\left\{1 - \frac{4ikc_W e^{-2k(d-g)}}{\omega[1-e^{-4k(d-g)}]}\right\}, \tag{48}$$

where

$$F_c = \frac{[1+e^{-2k(d-g)}]}{[1-e^{-2k(d-g)}]}. \tag{49}$$

Substituting Eq. (48) into Eq. (40), the symmetric dispersion relation becomes

$$\frac{kg}{\beta g}F_c - \tan \beta g \simeq \frac{4ikc_W e^{-2k(d-g)}}{\omega[1-e^{-4k(d-g)}]}\frac{kgF_c}{\beta g}. \tag{50}$$

For $kc_W/\omega = 0$, the unperturbed roots of Eq. (50) are denoted by

$$\beta g = a_n. \tag{51}$$

Hence, from Eq. (39), the unperturbed frequencies of the symmetric Alfvén modes are given by

$$\frac{(\bar{\omega}^2-k^2c_A^2)g^2}{c_A^2}=a_n^2. \tag{52}$$

Thus, the solutions are

$$\omega=kv_0\pm kc_A\left(1+\frac{a_n^2}{k^2g^2}\right)^{1/2}, \tag{53}$$

where the $\pm$ signs correspond to the fast and slow compressional Alfvén waves of the bounded system. For small values of the parameter kc_W/ω, a perturbation solution of Eq. (50) is sought. Assuming

$$\omega=kv_0-kc_A\left(1+\frac{a_n^2}{k^2g^2}\right)^{1/2}+\delta\omega \tag{54}$$

the perturbed value of βg is first obtained, giving

$$\beta g\simeq a_n\left\{1-\frac{k^2g^2}{a_n^2}\left(1+\frac{a_n^2}{k^2g^2}\right)^{1/2}\frac{\delta\omega}{kc_A}\right\} \tag{55}$$

and substituting Eqs. (54) and (55) into Eq. (50), the perturbed frequency $\delta\omega$ is obtained

$$\frac{\delta\omega}{kc_A}\simeq\frac{4ikc_We^{-2k(d-g)}(kg/a_n)F_c}{[kv_0-kc_A(1+(a_n^2/k^2g^2))^{1/2}][1-e^{-4k(d-g)}](k^2g^2/a_n^2)(1+(a_n^2/k^2g^2))^{1/2}[(kg/a_n)F_c+a_n\sec^2 a_n]}. \tag{56}$$

Hence, the slow compressional Alfvén wave is unstable when

$$v_0>c_A\left(1+\frac{a_n^2}{k^2g^2}\right)^{1/2}.$$

The growth rate is again proportional to the wall resistivity but the mode now oscillates at the frequency of the slow Alfvén wave. This instability is analogous to the resistive wall amplifier of Birdsall *et al.*[9] The interpretation of this instability is that the slow Alfvén wave is a negative energy mode when $v_0>c_A(1+a_n^2/k^2g^2)^{1/2}$. Hence, due to the dissipation provided by the resistive wall, the wave is caused to grow.

With the aid of this interpretation, Eq. (42) for the symmetric mode can be analyzed in the vicinity of a zero of the denominator. For this purpose, Eq. (42) is written in the form

$$\omega\left(\frac{kg}{\beta g}-\frac{\tan\beta g}{F_c}\right)=-\frac{2ikc_W[(kg/\beta g)-\tan\beta g]}{[1+e^{-2k(d-g)}]}. \tag{57}$$

It has just been noted that the zeros of the bracket on the left-hand side of Eq. (57),

$$\frac{kg}{\beta g}-\frac{\tan\beta g}{F_c}=0 \tag{58}$$

describe the fast and slow compressional Alfvén waves. The critical condition for the slow wave occurs when the frequency of this mode passes through zero, corresponding to a change in sign of the energy. Hence, a perturbation solution of Eq. (57) is sought in which the equation is expanded about the value $\beta=\beta_0$ for which the slow wave has zero frequency. Thus, substituting $\beta=\beta_0$ in the right-hand side of Eq. (57), the equation describes the coupling of the zero frequency wall mode with the zero frequency slow Alfvén wave. For $kg=1$, $kd=1.5493$ a graphical solution of Eq. (58) gives the value $\beta_0=1.06$. The flow corresponding to a zero frequency slow Alfvén wave is $v_0=1.46c_A$. Hence, again making use of Eqs. (54) and (55) and expanding Eq. (57) about $\beta g=\beta_0 g$, the equation becomes

$$(\delta\omega)^2\simeq i\gamma^2, \tag{59}$$

where

$$\gamma^2=\frac{2kc_Wkc_A[\tan\beta_0 g-(kg/\beta_0 g)]}{[1+e^{-2k(d-g)}](k^2g^2/\beta_0^2g^2)[1+(\beta_0^2g^2/k^2g^2)]^{1/2}[(kg/\beta_0 g)+(\beta_0 g/F_c)\sec^2\beta_0 g]}, \tag{60}$$

and Eq. (58) has again been used to obtain Eq. (59). Hence, the solution of Eqs. (42) or (57) in the vicinity of $\beta=\beta_0$ is given approximately by

$$\delta\omega\simeq\pm\frac{\gamma}{\sqrt{2}}(1+i). \tag{61}$$

A numerical solution of Eq. (37) is given in Figs. 3(a)

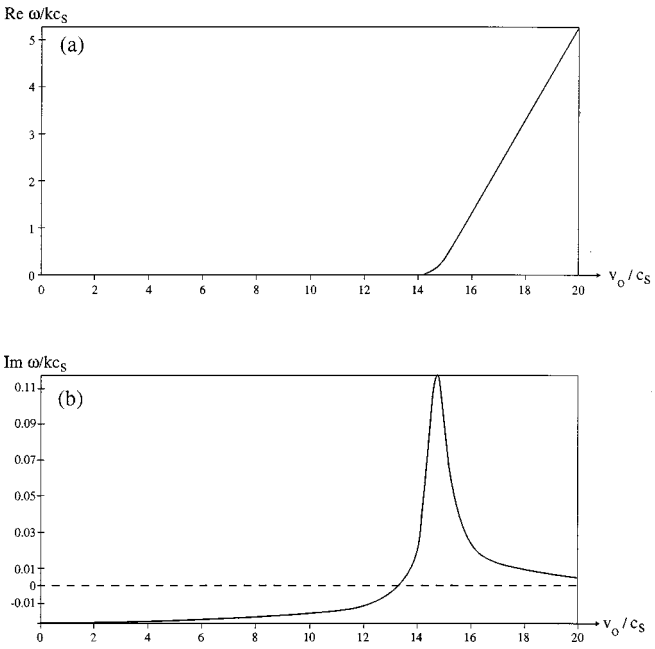

FIG. 3. Alfvén wave instability for the parameters $kg=1$, $kd=1.5493$, $c_W/c_s=0.01$, and $c_A/c_s=10$, (a) Re ω/kc_s vs v_0/c_S, (b) Im ω/kc_s vs v_0/c_s.

and 3(b). The growth rate and frequency normalized to kc_s are plotted as a function of the normalized flow velocity v_0/c_s. It can be seen that close to the threshold, the real part of the frequency is very small, which is characteristic of the wall mode. For velocities a little beyond that corresponding to maximum growth the frequency corresponds to the slow Alfvén wave value given by the negative sign in Eq. (53). The growth rate as a function of the flow velocity rises to a maximum just above the threshold and then falls off as v_0^{-1} in agreement with the perturbation result given by Eq. (56). Substituting the values of the parameters used to compute Figs. 3(a) and 3(b) into Eq. (61) yields the value $\omega/kc_s=0.12(1+i)$ which is in very good agreement with the computed values corresponding to maximum growth, given in Figs. 3(a) and 3(b). Similarly, Eq. (56) yields $\omega/kc_s=5.4+0.0064i$ for $v_0/c_A=2$ which is again seen to be in excellent agreement with the numerical values.

This behavior suggests the possibility of a corresponding instability associated with the slow magnetosonic wave of a compressible plasma, except that the critical velocity would be associated with the much smaller sound speed rather than the Alfvén speed.

B. Sound wave case

Returning to the form of the dispersion relation given by Eq. (37) (the symmetric modes) and assuming $\bar{\omega}\ll kc_A$, the equation becomes

$$\frac{\beta g}{kg}\simeq\frac{\tan\beta g}{G_c}. \tag{62}$$

Substituting Eq. (29) for G_c into Eq. (62) and proceeding as for Sec. IV A, we obtain a solution of ω which is valid in the vicinity of the marginal condition, $\omega=0$. Thus,

$$\omega=\frac{-2ikc_W[(\beta g/kg)+\tan\beta g]}{[1+e^{-2k(d-g)}]\{(\beta g/kg)+([1-e^{-2k(d-g)}]/[1+e^{-2k(d-g)}])\tan\beta g\}}, \tag{63}$$

where c_s^2 has again been neglected in comparison with c_A^2. The marginal condition is again given by the zeros of the numerator,

$$\frac{\beta g}{kg}+\tan\beta g=0. \tag{64}$$

Choosing $kg=1$, the marginal condition is given approximately by $v_0=c_s$. For values of βg just below the threshold value given by Eq. (64) we again have instability with a growth rate proportional to kc_W. As for the previous case the growth rate becomes infinitely large when the denominator for Eq. (63) becomes zero.

For the antisymmetric modes, Eq. (38), the low frequency assumption, $\bar{\omega}\ll kc_A$ reduces the dispersion relation to

$$-\frac{kg}{\beta g}=G_c\tan\beta g. \tag{65}$$

Substituting for G_c from Eq. (29), the solution for ω which is valid in the vicinity of the marginal condition, $\omega=0$, is given by

$$\omega=\frac{-2ikc_W[(kg/\beta g)-\tan\beta g]}{[1-e^{-2k(d-g)}]\{(kg/\beta g)-([1+e^{-2k(d-g)}]/[1-e^{-2k(d-g)}])\tan\beta g\}}. \tag{66}$$

The threshold condition is therefore

$$\frac{kg}{\beta g}-\tan\beta g=0, \tag{67}$$

which, for $kg=1$, also yields the marginal condition $v_0=c_s$. The antisymmetric mode is unstable for values of βg just above the threshold value given by Eq. (64) with a growth rate proportional to kc_W.

We note that the approximate analysis of the sound instability neglects terms $0(c_s^2/c_A^2)$. Hence, the threshold velocities for the symmetric and antisymmetric modes are the same.

Now consider the significance of the infinite growth rates arising from the zeros of the denominators in Eqs. (63) and (66). It is convenient to analyze the antisymmetric mode in this case. Thus, the approximate form of G_c for $kc_W/\omega \ll 1$ given by Eq. (48) is substituted into Eq. (65), yielding

$$\frac{kg}{\beta g}-F_c\tan\beta g=\frac{-4ikc_We^{-2k(d-g)}}{\omega[1-e^{-4k(d-g)}]}F_c\tan\beta g. \tag{68}$$

A perturbation solution of Eq. (68) is now sought. For $kc_W/\omega=0$, the unperturbed solution of Eq. (68) is denoted by

$$\beta g=b_n \tag{69}$$

and the unperturbed frequencies are

$$\omega=kv_0\pm kc_s\alpha, \tag{70}$$

where

$$\alpha^2=\frac{(1+b_n^2/k^2g^2)}{[1+b_n^2/k^2g^2+(b_n^2/k^2g^2)(c_s^2/c_A^2)]}. \tag{71}$$

The $\pm$ solutions, Eq. (70), are referred to as the fast and slow sound waves. Looking for a perturbation solution of Eq. (68), we take

$$\omega\simeq kv_0-kc_s\alpha+\delta\omega. \tag{72}$$

Substituting Eq. (72) into Eq. (8) and using the condition $\overline{\omega}^2\ll k^2c_A^2$, the perturbed form of βg is

$$\beta g\simeq b_n\left\{1+\frac{2c_A^2}{c_s^2}\frac{(k^2g^2+b_n^2)^2}{k^2g^2b_n^2}\frac{\delta\omega}{kc_s}\right\}. \tag{73}$$

Substituting Eqs. (72) and (73) into Eq. (68), the resulting correction to the slow sound wave frequency is obtained

$$\frac{\delta\omega}{kc_s}\simeq\frac{4ikc_We^{-2k(d-g)}F_c(c_s^2/2c_A^2)k^2g^2b_n^2\tan b_n}{k(v_0-\alpha c_s)[1-e^{-4k(d-g)}](k^2g^2+b_n^2)^2[(kg/b_n)+F_cb_n\sec^2 b_n]}. \tag{74}$$

Hence, the slow sound wave is unstable when $v_0>\alpha c_s$ where α is approximately unity. The behavior of the sound-type resistive wall instability is similar to the Alfvén case. Thus, very close to the threshold velocity, $v_0=c_s$, the instability has a very low frequency characteristic of the wall mode, with a growth rate proportional to the wall resistivity. The maximum growth occurs when the zero frequency wall mode couples to the zero frequency slow sound wave. For velocities just above the velocity at which maximum growth occurs, the instability is associated with the slow sound wave, oscillating with the frequency of this mode. For the sound wave case, the coupling of the slow sound wave with the wall mode occurs much closer to the threshold than for the Alfvén case. In order to carry out an analytic calculation of the behavior of the instability at maximum growth, the analysis would need to include the previously neglected terms, $0(c_s^2/c_A^2)$. For this case we give just the numerical solution of the antisymmetric dispersion relation. The results are shown in Fig. 4(a) (real part of ω/kc_s) and Fig. 4(b) (imaginary part of ω/kc_s) as a function of the normalized flow velocity v_0/c_s.

V. THE EFFECT OF LANDAU DAMPING

The resistive wall instability discussed in Sec. IV B is associated with the slow magnetosonic wave and occurs when the flow speed exceeds the sound speed. Such flows are relevant to the present generation of tokamaks. However, the ideal MHD model used in the previous section does not include dissipation. The condition for weakly damped sound waves is $T_e\gg T_i$, whereas under normal tokamak conditions, $T_e\sim T_i$, when the slow magnetosonic mode undergoes strong ion Landau damping.

In view of this we introduce Landau damping into our model. Since the dominant kinetic effects for the slow magnetosonic mode are due to the thermal motion parallel to the equilibrium magnetic field, we take advantage of our uniform slab model to incorporate the parallel kinetic effects in an approximate manner. We ignore the effect of the boundaries on the electron and ion distribution functions. Instead, we use the dielectric tensor for a hot, uniform plasma to obtain a generalization of Eq. (6) for the perturbed magnetic field. We also need to include kinetic effects in the perturbed pressure, given by Eq. (21).

The equation describing the perturbed magnetic field component B_{1x}, can be obtained from Maxwell's equations and the hot plasma dielectric tensor for a uniform plasma. Following Shafranov[10] we obtain, for low frequencies ($\omega \ll \Omega_i$),

$$\begin{pmatrix} n_\parallel^2-\epsilon_{xx} & 0 & 0 \\ 0 & n^2-\epsilon_{yy} & -\epsilon_{yz} \\ 0 & \epsilon_{yz} & n_\perp^2-\epsilon_{zz} \end{pmatrix}\begin{pmatrix} E_{1x} \\ E_{1y} \\ E_{1z} \end{pmatrix}=0, \tag{75}$$

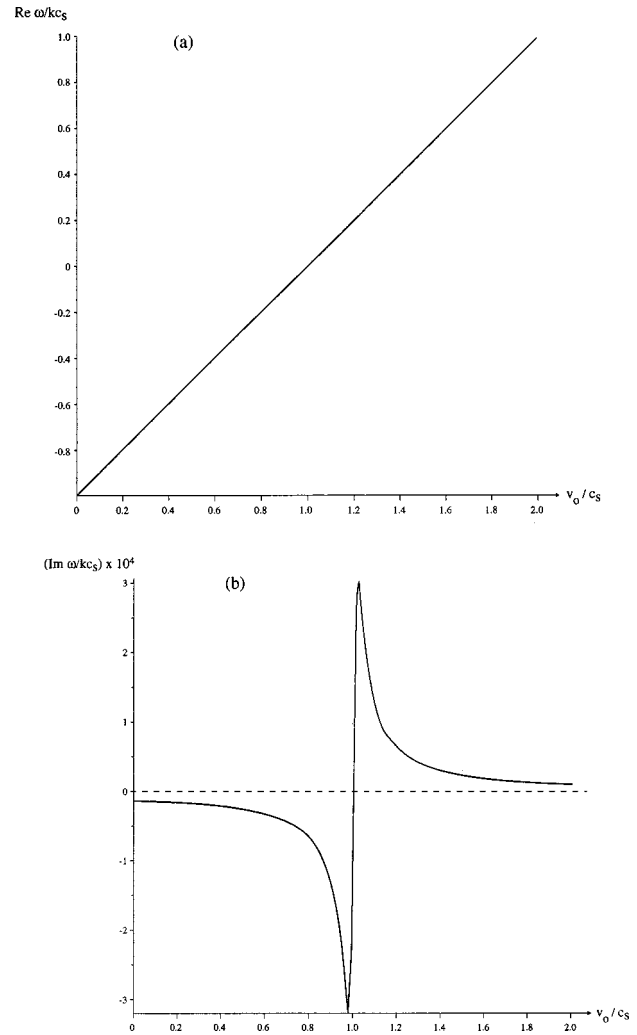

FIG. 4. Sound wave instability for the same parameters as Fig. 3, (a) Re ω/kc_s vs v_0/c_s, (b) Im ω/kc_s vs v_0/c_s.

where $n^2=n_\perp^2+n_\parallel^2$, $n_\perp^2=c^2k_\perp^2/\omega^2$ and $n_\parallel^2=c^2k^2/\omega^2$. As before, the shear Alfvén wave, $(n_\parallel^2-\epsilon_{xx})E_{1x}=0$, decouples from the fast and slow magnetosonic waves, described by

$$(n^2-\epsilon_{yy})E_{1y}-\epsilon_{yz}E_{1z}=0, \tag{76}$$

$$\epsilon_{yz}E_{1y}+(n_\perp^2-\epsilon_{zz})E_{1z}=0. \tag{77}$$

For low frequencies, $n_\perp^2 \ll \epsilon_{zz}$, when Eq. (77) yields

$$E_{1z}\simeq \frac{\epsilon_{yz}E_{1y}}{\epsilon_{zz}}. \tag{78}$$

Hence, from Eqs. (76) and (78),

$$\left(n_\perp^2+n_\parallel^2-\epsilon_{yy}-\frac{\epsilon_{yz}^2}{\epsilon_{zz}}\right)E_{1y}=0. \tag{79}$$

The dielectric tensor elements for the low frequency case can be approximated by (see, for example, Stix[11] and Swanson[12]),

$$\epsilon_{yy}\simeq \frac{\omega_{pi}^2}{\Omega_i^2}\equiv\frac{c^2}{c_A^2}, \tag{80}$$

$$\epsilon_{yz}\simeq \frac{i\omega_{pi}^2}{\omega\Omega_i}\frac{k_\perp}{k}[1+\zeta_iZ(\zeta_i)]-\frac{i\omega_{pe}^2}{\omega\Omega_e}\frac{k_\perp}{k}[1+\zeta_eZ(\zeta_e)], \tag{81}$$

$$\epsilon_{zz}\simeq 1+\frac{2\omega_{pi}^2}{k^2v_{Ti}^2}[1+\zeta_iZ(\zeta_i)]+\frac{2\omega_{pe}^2}{k^2v_{Te}^2}[1+\zeta_eZ(\zeta_e)], \tag{82}$$

where $\zeta_j=\omega/kv_{Tj}$, ''j'' denotes either ions or electrons, $v_{Tj}=(2T_j/m_j)^{1/2}$, and $Z(\zeta_j)$ is the plasma dispersion function.

For sound wave frequencies, $\zeta_e \ll 1$ and $\zeta_i \gg 1$ if $T_e \gg T_i$. When $T_i \sim T_e$, $\zeta_i \sim 1$. Hence we retain the full plasma dispersion function for the ions in $\epsilon_{yz}, \epsilon_{zz}$ but neglect the very weak electron Landau damping since $\zeta_e \ll 1$. Under these conditions, Eqs. (81) and (82) can be further approximated to

$$\epsilon_{yz}\simeq \frac{i\omega_{pi}^2}{\omega\Omega_i}\frac{k_\perp}{k}\zeta_iZ(\zeta_i), \tag{83}$$

$$\epsilon_{zz}\simeq \frac{2\omega_{pi}^2}{k^2v_{Ti}^2}\left[1+\zeta_iZ(\zeta_i)+\frac{T_i}{T_e}\right]. \tag{84}$$

Substituting Eqs. (83) and (84) into Eq. (79), we obtain

$$k_\perp^2E_{1y}-\frac{(\omega^2-k^2c_A^2)[1+\zeta_iZ(\zeta_i)+(T_i/T_e)]}{\{c_A^2[1+\zeta_iZ(\zeta_i)+(T_i/T_e)]+(v_{Ti}^2/2)\,\zeta_i^2Z^2(\zeta_i)\}}E_{1y}=0. \tag{85}$$

Taking the inverse Fourier transform and using the Maxwell equation, $B_{1x}=-(k/\omega)E_{1y}$, we obtain the generalization of Eq. (6),

$$\frac{d^2B_{1x}}{dx^2}+\frac{(\omega^2-k^2c_A^2)[1+\zeta_iZ(\zeta_i)+(T_i/T_e)]}{\{c_A^2[1+\zeta_iZ(\zeta_i)+(T_i/T_e)]+(v_{T_i}^2/2)\,\zeta_i^2Z^2(\zeta_i)\}}B_{1x}=0. \tag{86}$$

In the limit $T_e \gg T_i$, where $\zeta_i \gg 1$, $1+\zeta_iZ(\zeta_i) \sim -k^2v_{T_i}^2/(2\omega^2)$, $\zeta_iZ(\zeta_i)\sim -1$, and Eq. (86) reduces to Eq. (6). Thus, Eq. (86) extends the previous model to include the effect of ion Landau damping.

To complete this extension of the MHD model we must also obtain the kinetic generalization of Eq. (21) for the perturbed pressure. The pressure tensor is given by

$$p=m_j\int (f_{0j}+f_{1j})(\mathbf{v}-\mathbf{u})(\mathbf{v}-\mathbf{u})d\mathbf{v}, \tag{87}$$

where $\mathbf{u}=\int(f_{0j}+f_{1j})\mathbf{v}d\mathbf{v}$.

We will simplify this calculation by assuming that the plasma is stationary with a Maxwellian distribution. In this case, $\int f_{0j}\mathbf{v}d\mathbf{v}=0$, so that $\mathbf{u}$ is a first order quantity in the perturbed amplitude and does not contribute to the perturbed pressure within a linear analysis. We must therefore evaluate

$$p_{1xx}^j=m_j\int f_{1j}v_x^2d\mathbf{v}. \tag{88}$$

We use the perturbed distribution function f_{1j} given by Swanson[12]

$$f_{1j}(\mathbf{k},\mathbf{v},\omega)=-\frac{iq_j}{m_j}\sum_{m=-\infty}^{\infty}\sum_{n=-\infty}^{\infty}\frac{J_m(b)e^{i(m-n)\phi}}{(\omega-\epsilon n\omega_{cj}-kv_z)}$$
$$\times\left\{\frac{nJ_n(b)}{b}\left[f_{0\perp}+\frac{k}{\omega}(v_\perp f_{0z}-v_z f_{0\perp})\right]E_{1x}\right.$$
$$+iJ_n'(b)\left[f_{0\perp}+\frac{k}{\omega}(v_\perp f_{0z}-v_z f_{0\perp})\right]E_{1y}$$
$$+J_n(b)\left[f_{0z}-\frac{\epsilon n\omega_{cj}}{\omega}(f_{0z}\right.$$
$$\left.\left.-(v_z/v_\perp)f_{0\perp})\right]E_{1z}\right\}, \tag{89}$$

where

$$f_{0\perp}\equiv\frac{\partial f_{0j}}{\partial v_\perp},\quad f_{0z}\equiv\frac{\partial f_{0j}}{\partial v_z},\quad b=\epsilon k_\perp v_\perp/\omega_{cj},$$
$$\epsilon=q_j/|q_j|,\quad \mathbf{k}=(k_\perp,0,k),$$
$$v_x=v_\perp\cos\phi\quad\text{and}\quad v_y=v_\perp\sin\phi.$$

The dominant contribution comes from the $n=0$ terms and is

$$p_{1xx}^j\simeq -iq_j\pi\int_{-\infty}^{\infty}\int_0^{\infty}v_\perp^3\left(-\frac{2}{b}J_0'(b)\right)$$
$$\times J_0(b)dv_\perp\frac{(\partial f_{0j}/\partial v_z)}{(\omega-kv_z)}dv_z E_{1z}, \tag{90}$$

where the integration over ϕ has been carried out. Assuming $|b|\ll 1$, and carrying out the remaining velocity–space integrations,

$$p_{1xx}^j=\frac{-iq_j n_{0j}E_{1z}}{k}[1+\zeta_j Z(\zeta_j)]. \tag{91}$$

Using Eq. (78) and the relation between E_{1y} and B_{1x},

$$E_{1z}=-\frac{\epsilon_{yz}}{\epsilon_{zz}}\frac{\omega}{k}B_{1x}. \tag{92}$$

Substituting Eq. (92) into Eq. (91),

$$p_{1xx}^j=\frac{iq_j n_{0j}}{k}\frac{\epsilon_{yz}}{\epsilon_{zz}}\frac{\omega}{k}[1+\zeta_j Z(\zeta_j)]B_{1x}. \tag{93}$$

Assuming cold ions for the moment and again using $\zeta_e\ll 1$ to neglect the weak electron Landau damping contribution,

$$p_{1xx}^e\simeq\frac{-ien_{0e}}{k}\frac{\epsilon_{yz}}{\epsilon_{zz}}\frac{\omega}{k}B_{1x}, \tag{94}$$

where e is the proton charge. For the conditions just stated, Eqs. (81) and (82) give

$$\frac{\epsilon_{yz}}{\epsilon_{zz}}\simeq-\frac{i}{2}\frac{k_\perp k v_{Te}^2\omega}{(\omega^2-k^2c_s^2)\Omega_e}. \tag{95}$$

Substituting Eq. (95) into Eq. (94) and using $k_\perp B_{1x}=-i(dB_{1x}/dx)$, we obtain

$$p_{1xx}^e\simeq\frac{i\rho_0\omega^2c_s^2}{kB_0^p(\omega^2-k^2c_s^2)}\frac{dB_{1x}}{dx}, \tag{96}$$

which is in agreement with Eq. (21), obtained from the MHD model.

Returning to the kinetic expression, Eq. (91), and now including the effect of hot ions, we write

$$p_{1xx}=\frac{ien_0E_{1z}}{k}-\frac{ien_0E_{1z}}{k}[1+\zeta_i Z(\zeta_i)], \tag{97}$$

where we have again neglected the weak electron Landau damping. For this case,

$$\frac{\epsilon_{yz}}{\epsilon_{zz}}\simeq\frac{(i\omega_{pi}^2/\omega\Omega_i)}{(2\omega_{pi}^2/k^2v_{Ti}^2)}\frac{(k_\perp/k)\,\zeta_i Z(\zeta_i)}{[1+\zeta_i Z(\zeta_i)+(T_i/T_e)]}. \tag{98}$$

Proceeding as before, we obtain

$$p_{1xx}=\frac{i}{2}\frac{\rho_0 v_{Ti}^2}{kB_0^p}\frac{\zeta_i^2Z^2(\zeta_i)}{[1+\zeta_i Z(\zeta_i)+(T_i/T_e)]}\frac{dB_{1x}}{dx}. \tag{99}$$

In the limit, $\zeta_i\gg 1$, Eq. (99) reduces to Eq. (21) obtained from the MHD model. We are now in a position to derive the generalization of the dispersion relation obtained in Sec. IV to include the effect of ion Landau damping. The procedure is identical to that used in Sec. IV except Eqs. (86) and (99) are used instead of Eqs. (6) and (21). The resulting dispersion relation is formally the same as before, Eq. (25), which factors into the symmetric, Eq. (30), and antisymmetric, Eq. (31), dispersion relations. The only difference is that the quantity F is no longer given by Eq. (28), but instead by

$$F=\frac{v_{Ti}^2\overline{\zeta_i^2}Z^2(\overline{\zeta_i})}{2[1+\overline{\zeta_i}Z(\overline{\zeta_i})+(T_i/T_e)]}+c_A^2 \tag{100}$$

and β^2 is now,

$$\beta^2=\frac{(\overline{\omega^2}-k^2c_A^2)[1+\overline{\zeta_i}Z(\overline{\zeta_i})+(T_i/T_e)]}{\{c_A^2[1+\overline{\zeta_i}Z(\overline{\zeta_i})+(T_i/T_e)]+(v_{Ti}^2/2)\overline{\zeta_i^2}Z^2(\overline{\zeta_i})\}}, \tag{101}$$

instead of Eq. (8). We note that the generalized equations for B_{1x}, Eq. (86), and the pressure p_{1xx}, Eq. (99), have been derived for a stationary plasma. In order to relate to Sec. IV, where the plasma is flowing, we have Doppler shifted the frequencies occurring in Eqs. (100) and (101). Thus, $\overline{\zeta_i}=(\omega-kv_0)/kv_{T_i}$ and $\overline{\omega}$ has already been defined after Eq. (5).

Let us now obtain solutions of the antisymmetric dispersion relation which is still given by Eq. (38), except that β^2 is now given by Eq. (101). For the slow magnetosonic (sound) wave case the dispersion relation again reduces to Eq. (65). We now consider this case under conditions where $T_e\gg T_i$ so that the ion Landau damping is weak and we can obtain a perturbation solution. First, we expand Eq. (101) asymptotically assuming $\overline{\zeta_i}\gg 1$,

$$\beta^2 \simeq \frac{-k^2c_A^2[\overline{\omega}^2 - k^2c_s^2 + i\pi^{1/2}\overline{\omega}^2\overline{\zeta}_i(T_e/T_i)e^{-\overline{\zeta}_i^2}]}{\{c_A^2[\overline{\omega}^2 - k^2c_s^2 + i\pi^{1/2}\overline{\omega}^2\overline{\zeta}_i(T_e/T_i)e^{-\overline{\zeta}_i^2}] + \overline{\omega}^2c_s^2[-1 + i\pi^{1/2}\overline{\zeta}_i e^{-\overline{\zeta}_i^2}]^2\}}. \tag{102}$$

β^2 is now in a very similar form to the expression given in Eq. (8) except that Eq. (102) contains the effect of weak ion Landau damping. In order to obtain a perturbation solution to Eq. (65) including the effect of ion Landau damping, we again assume that $kc_w \ll 1$ and use the approximation to G_c given in Eq. (48). Thus, treating both kc_w and the ion Landau damping as small perturbations to the antisymmetric dispersion relation, the unperturbed equation is given by the left-hand side of Eq. (68) and the unperturbed frequencies of the fast and slow sound waves are as shown in Eq. (70). Substituting the perturbed slow sound wave solution, Eq. (72), into Eq. (102), we obtain the perturbed value of βg due to the presence of the resistive wall perturbation and weak damping,

$$\beta g \simeq b_n\left(1 + A\frac{\delta\omega}{kc_s} + i\delta\right), \tag{103}$$

where b_n are the roots of the unperturbed equation

$$A = \frac{\alpha}{(1-\alpha^2)} + \frac{\alpha[1 + (c_s^2/c_A^2)]}{[\alpha^2 + \alpha^2(c_s^2/c_A^2) - 1]}, \tag{104}$$

and

$$\delta = -\pi^{1/2}\left\{\frac{\alpha^2}{(1-\alpha^2)}\frac{T_e}{2T_i} + \frac{\alpha^2}{[\alpha^2 + \alpha^2(c_s^2/c_A^2) - 1]} \times\left(\frac{T_e}{2T_i} - \frac{c_s^2}{c_A^2}\right)\right\}\overline{\zeta}_i e^{-\overline{\zeta}_i^2}. \tag{105}$$

Substituting Eqs. (48) and (103) into Eq. (65), we obtain the perturbed dispersion relation,

$$\frac{kg}{b_n[1 + A(\delta\omega/kc_s) + i\delta]} - F_c\tan\left[b_n\left(1 + A\frac{\delta\omega}{kc_s} + i\delta\right)\right] \simeq -\frac{4ikc_We^{-2k(d-g)}}{(kv_0 - kc_s\alpha)[1 - e^{-4k(d-g)}]}F_c\tan b_n, \tag{106}$$

where only the unperturbed values of ω and βg have been substituted into the term proportional to kc_W, since this is a perturbation. Expanding the terms on the left-hand side of Eq. (106) for small $\delta\omega/kc_s$ and small δ, we obtain

$$\frac{kg}{b_n}\left(1 - A\frac{\delta\omega}{kc_s} - i\delta\right) - F_c\tan b_n - F_c b_n\left(A\frac{\delta\omega}{kc_s} + i\delta\right)\sec^2 b_n = -\frac{4ikc_We^{-2k(d-g)}F_c\tan b_n}{(kv_0 - kc_s\alpha)[1 - e^{-4k(d-g)}]}. \tag{107}$$

Making use of the unperturbed equation, $(kg/b_n) - F_c\tan b_n = 0$, Eq. (107) yields the solution for $\delta\omega$,

$$\frac{\delta\omega}{kc_s} \simeq \frac{4ikc_We^{-2k(d-g)}F_c\tan b_n}{(kv_0 - kc_s\alpha)[1 - e^{-4k(d-g)}]A[(kg/b_n) + b_nF_c\sec^2 b_n]} - \frac{i\delta}{A}. \tag{108}$$

Substituting Eqs. (104) and (105) into Eq. (108) and the result $\overline{\zeta}_i \simeq -(T_e/2T_i)$, we obtain the final form for $\delta\omega$,

$$\frac{\delta\omega}{kc_s} \simeq \frac{4ikc_We^{-2k(d-g)}F_c(c_s^2/2c_A^2)k^2g^2b_n^2\tan b_n}{k(v_0 - \alpha c_s)[1 - e^{-4k(d-g)}](k^2g^2 + b_n^2)^2[(kg/b_n) + b_nF_c\sec^2 b_n]} - \frac{i\pi^{1/2}}{2}\left(\frac{T_e}{2T_i}\right)^{3/2}e^{-(T_e/2T_i)}. \tag{109}$$

Hence, as T_e/T_i decreases, the ion Landau damping term becomes stronger and for some critical value the growth rate will be zero. For still smaller values of T_e/T_i the resistive wall instability associated with the slow sound wave becomes stable.

This behavior is illustrated in Figs. 5–7 in which numerical solutions of the exact dispersion relation, Eq. (38) with β^2 given by Eq. (101), are displayed. In Fig. 5, the normalized growth rate is plotted as a function of v_{Ti}/c_s for $v_0/c_s = 1.5$. As v_{Ti}/c_s increases (or equivalently, as T_e/T_i decreases) the growth rate also decreases and passes through zero when $v_{Ti}/c_s \simeq 0.275$. This gives the critical value (referred to above) $T_e/T_i \simeq 26$ for the parameters used. This is in reasonable agreement with Eq. (109) which yields a critical value $T_e/T_i \simeq 30$ for the same parameters. As v_{Ti}/c_s increases further, the mode becomes more and more strongly damped, as shown in Fig. 6.

In the absence of damping (cf. Fig. 4), the growth rate of the slow sound wave takes on its maximum value when v_0 is close to c_s. Since Figs. 5 and 6 were obtained for v_0

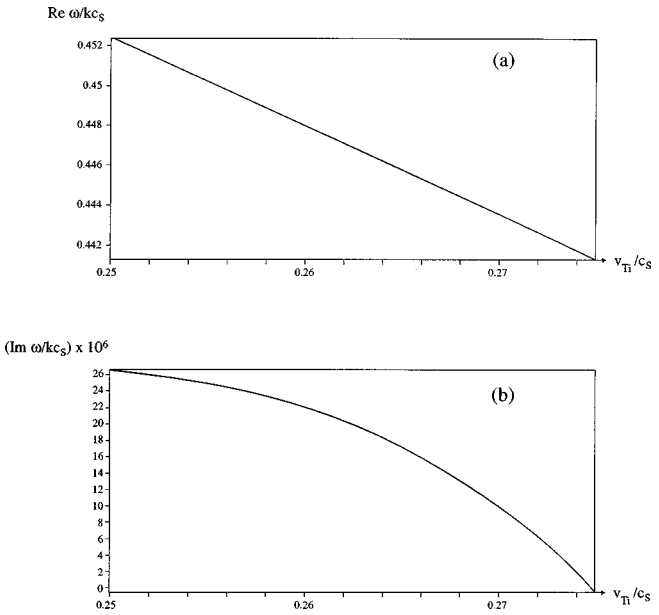

FIG. 5. Sound wave instability with ion Landau damping for same parameters as Fig. 3, (a) Re ω/kc_s vs v_{Ti}/c_s, (b) Im ω/kc_s vs v_{Ti}/c_s near to the stability boundary.

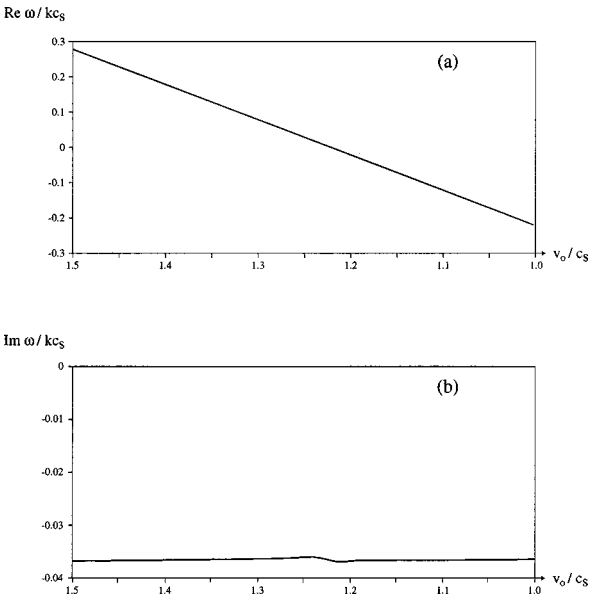

FIG. 7. Sound wave with ion Landau damping for same parameters as Fig. 3, (a) Re ω/kc_s vs v_0/c_s, (b) Im ω/kc_s vs v_0/c_s.

$=1.5c_s$, well away from the region of maximum growth, we have also solved the dispersion relation for the real and imaginary parts of the normalized frequency of the slow sound wave for $v_{Ti}/c_s=0.5$ $(T_e/T_i=8)$ as a function of v_0/c_s. The results are shown in Fig. 7 and it can be seen that the damping rate is now almost constant over the range of v_0/c_s from 1 to 1.5, apart from a very small variation around $v_0 \simeq 1.2c_s$.

VI. SUMMARY AND CONCLUSIONS

A sharp boundary, uniform plasma with a uniform flow along the magnetic field, separated from a resistive wall by a vacuum region, has been shown to be subject to two instabilities both of which depend on the wall resistance and the flow. The first instability has a threshold velocity, $v_0 \gtrsim c_A$, a case which has recently been analyzed by Wesson.[8] This instability is associated with the slow, compressional Alfvén wave and a resistive wall mode.

The second instability has a threshold, $v_0 \simeq c_s$ and is associated with the slow sound wave and a resistive wall mode and clearly requires the effect of plasma compressibility. In both cases, the unstable mode changes its character from a zero frequency resistive wall mode close to the threshold to an oscillatory mode when the flow speed is somewhat above the threshold value. The maximum growth rates occur when the zero frequency wall mode couples to the zero frequency slow wave (Alfvén or sound). Under these circumstances the behavior is more characteristic of a reactive or ideal instability than of a dissipative or resistive one. The oscillatory instabilities, slow Alfvén or slow sound, are analogous to the resistive wall amplifier proposed by Birdsall *et al.*[9]

In the final part of the above analysis the slow sound instability has been generalized to include the effect of ion Landau damping. This was because the slow magnetosonic wave is normally strongly damped by ion Landau damping when $T_i \sim T_e$. It was found that since the growth rate of the resistive wall/slow magnetoacoustic instability is rather small it is stabilized by weak ion Landau damping. For strong ion Landau damping, the damping rate of the slow sound wave is almost independent of the flow speed, above or below the sound speed. The inclusion of kinetic ion damping suggests a possible interpretation of the stabilizing effect of plasma flow.

In the absence of flow, the resistive wall instability occurs at zero frequency and hence would be insensitive to ion Landau damping. It is now clear that the presence of flow could introduce a damping mechanism to the wall mode by

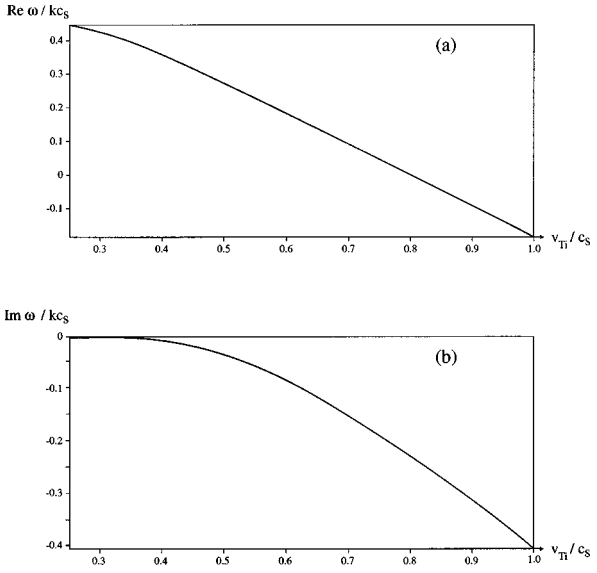

FIG. 6. Sound wave with ion Landau damping for same parameters as Fig. 3, (a) Re ω/kc_s vs v_{Ti}/c_s, (b) Im ω/kc_s vs v_{Ti}/c_s.

Doppler shifting ions into wave-particle resonance with the mode. In order to produce a noticeable effect, the flow speed should be a significant fraction of the ion thermal speed.

For the idealized model considered in this paper, the only source of free energy is the flow itself. It would therefore be of interest to extend the treatment presented to a more realistic model in which free magnetic energy is present.

ACKNOWLEDGMENTS

This work is jointly funded by the United Kingdom Department of Trade and Industry and EURATOM.

[1]T. S. Taylor, E. J. Strait, L. Lao *et al.*, Phys. Plasmas **2**, 2390 (1995).
[2]A. Bondeson and D. Ward, Phys. Rev. Lett. **72**, 2709 (1994).
[3]R. Betti and J. P. Freidberg, Phys. Rev. Lett. **74**, 2949 (1995).
[4]J. M. Finn, Phys. Plasmas **2**, 198 (1995).
[5]M. S. Chu, J. M. Greene, T. H. Jensen, R. L. Miller, A. Bondeson, R. W. Johnson, and M. E. Maul, Phys. Plasmas **2**, 2236 (1995).
[6]R. Fitzpatrick and A. Aydemir, Nucl. Fusion **36**, 11 (1996).
[7]C. G. Gimblett, Nucl. Fusion **26**, 617 (1986).
[8]J. A. Wesson, Phys. Plasmas **5**, 3816 (1998)
[9]C. K. Birdsall, G. R. Brewer, and A. V. Haeff, Proc. IRE **41**, 865 (1953).
[10]V. D. Shafranov, Rev. Plasma Phys. **3**, 93 (1967).
[11]T. H. Stix, *Waves in Plasmas* (American Institute of Physics, New York, 1992), p. 257.
[12]D. G. Swanson, *Plasma Waves* (Academic, Boston, 1989), p. 146 and 155–156.